

An Optimal Control Method for Reconstruction of Topography in Dam-Break Flows

Alia Alghosoun, Nabil El Moçayd, Mohammed Seaid

Abstract—Modeling dam-break flows over non-flat beds requires an accurate representation of the topography which is the main source of uncertainty in the model. Therefore, developing robust and accurate techniques for reconstructing topography in this class of problems would reduce the uncertainty in the flow system. In many hydraulic applications, experimental techniques have been widely used to measure the bed topography. In practice, experimental work in hydraulics may be very demanding in both time and cost. Meanwhile, computational hydraulics have served as an alternative for laboratory and field experiments. Unlike the forward problem, the inverse problem is used to identify the bed parameters from the given experimental data. In this case, the shallow water equations used for modeling the hydraulics need to be rearranged in a way that the model parameters can be evaluated from measured data. However, this approach is not always possible and it suffers from stability restrictions. In the present work, we propose an adaptive optimal control technique to numerically identify the underlying bed topography from a given set of free-surface observation data. In this approach, a minimization function is defined to iteratively determine the model parameters. The proposed technique can be interpreted as a fractional-stage scheme. In the first stage, the forward problem is solved to determine the measurable parameters from known data. In the second stage, the adaptive control Ensemble Kalman Filter is implemented to combine the optimality of observation data in order to obtain the accurate estimation of the topography. The main features of this method are on one hand, the ability to solve for different complex geometries with no need for any rearrangements in the original model to rewrite it in an explicit form. On the other hand, its achievement of strong stability for simulations of flows in different regimes containing shocks or discontinuities over any geometry. Numerical results are presented for a dam-break flow problem over non-flat bed using different solvers for the shallow water equations. The robustness of the proposed method is investigated using different numbers of loops, sensitivity parameters, initial samples and location of observations. The obtained results demonstrate high reliability and accuracy of the proposed techniques.

Keywords—Optimal control, ensemble Kalman Filter, topography reconstruction, data assimilation, shallow water equations.

I. INTRODUCTION

BED topography has a detrimental impact on many applications in hydraulics widely modeled using the well-established shallow water equations. These models require prior information on the bed topography to be solvable and consequently, resolve the flow features in the problem under study. Experimental measurements have been used in

many hydraulic applications to reconstruct bathymetry in free-surface flows. However, this may be limited with time, cost and also geographical restrictions which need to be replaced with fast, easy to implement and cost effective computational techniques. In recent years, many research studies have been carried out to accurately describe and predict geophysical flows. This includes predicting floods, monitoring river flows, and predicting Tsunami waves, see for example [12], [8], [15]. Accurate numerical modeling of this class of free-surface flows and predicting flood inundation, all depends on the accurate representation of the bed topography. Authors in [11] have investigated the quality of the bathymetric airborne LiDAR survey. Information about the river bed geometry from top sight has also investigated in [22]. In a slightly different context, authors in [23] have studied the inverse problem of reconstructing the substrate topography from known data at the free surface. On the other hand, there have been significant developments in experimental techniques to measure river bathymetry and flow depths. For instance, the interferometric synthetic aperture radar (SAR) digital photogrammetry has been described in [29]. However, most experimental techniques to identify the bed elevation can be expensive and time consuming, see for example [13], [25].

From a numerical view point, there are mainly two different approaches for bed reconstruction in hydraulics namely, the direct approach and the optimization-based approach. The direct approach of the inverse problem is not a common way in the literature. In this method, the governing equations of the forward problem are used in the model rearrangement. In practice, the process depends on the determination of observable parameters in the analysis of the forward problem. However, this approach is not always possible and it is restricted to some inverse problems. For example, authors in [10], [1] have implemented this approach to determine the bed elevation from known data in open channel and Glacier flows. The optimization-based approach is well known for solving these types of inverse problems in computational hydraulics. In this approach, a minimization function is formulated and used to iteratively determine the model parameters. This iterative procedure has been implemented in [6], [18], [20], to determine the topography and the bed roughness for several hydraulic problems.

In the current study, we aim to tackle problems of bed reconstruction in shallow water flows using adaptive control Ensemble Kalman Filter (EnKF). The reconstruction is carried out based on given observation data at the free surface for the water depth. The main focus is on dam-break problems over non-flat beds for which the topography

A. Alghosoun is with Department of Engineering, University of Durham, South Road, Durham DH1 3LE, UK (e-mail: alia.r.al-ghosoun@durham.ac.uk).

N. El Moçayd is with International Water Research Institute, University Mohammed VI Polytechnic, 43150 Benguerir, Morocco (e-mail: nabil.elmocayd@um6p.ma).

M. Seaid is with Department of Engineering, University of Durham, South Road, Durham DH1 3LE, UK (e-mail: m.seaid@durham.ac.uk).

required reconstruction. The governing equations consist of the conservation system of shallow water equations accounting for bathymetric effects. As direct numerical solvers, we consider several finite volume schemes widely used in the literature to solve shallow water equations. The purpose is to examine the performance of the optimal control method for different solvers of the direct problem. Computational results are presented for various tests on a dam-break problem over non-flat topography. We also examine sensitivity of the method on different inputs including the initial guess and the uncertainty of observations. Numerical results presented in this study demonstrate high resolution of the proposed method and confirm its capability to provide highly accurate solutions for bed reconstruction in shallow water flows.

This paper is structured as follows: Modeling dam-break problems is discussed in Section II. This section introduces the shallow water equations used for the modeling and the finite volume schemes used for the numerical solution. Section III presents the proposed adaptive control Ensemble Kalman Filter (EnKF) for bed reconstruction. This section includes an overview of the EnKF in data assimilation and the implementation of the method for bed reconstruction in dam-break problems. Numerical results are discussed in Section IV. We present numerical results for a wide range of input parameters. Section V contains concluding remarks.

II. MODELING DAM-BREAK FLOWS OVER NON-FLAT BEDS

The well-established shallow water equations are considered in this study to model dam-break flows over non-flat beds. These equations can be derived by depth-averaging the incompressible Navier-Stokes equations and neglecting the vertical acceleration of water particles while the pressure is assumed hydrostatic, see [27] among others. In one space dimension, the shallow water equations read:

$$\begin{aligned} \frac{\partial h}{\partial t} + \frac{\partial(hu)}{\partial x} &= 0, \\ \frac{\partial(hu)}{\partial t} + \frac{\partial}{\partial x} \left(hu^2 + \frac{1}{2}gh^2 \right) &= -gh \frac{\partial B}{\partial x} - gh\tau_f, \end{aligned} \quad (1)$$

where t is the time variable, x the space coordinate, $h(x, t)$ the water depth, $u(x, t)$ the water velocity, g the gravitational constant and $B(x)$ the bed topography. In (1), τ_f is the friction slope term, which models effects of the bottom friction using the Manning empirical:

$$\tau_f = M_b^2 \frac{u|u|}{h^{4/3}}, \quad (2)$$

where is M_b the Manning roughness coefficient on the bed. To be consistent with a dam-break problem, (1) are equipped with following initial condition:

$$h(x, 0) = \begin{cases} h_l, & x \leq x_0, \\ h_r, & x > x_0 \end{cases} \quad (3)$$

where x_0 is the location of the dam, h_l and h_r are the water heights at upstream and downstream of the dam. Equations

(1)-(3) have been widely used in the literature to simulate dam-break problems, see for example [9], [3].

For simplicity in the representation, we reformulate (1) in a conservative form as:

$$\frac{\partial \mathbf{W}}{\partial t} + \frac{\partial \mathbf{F}(\mathbf{W})}{\partial x} = \mathbf{Q}(\mathbf{W}) + \mathbf{S}(\mathbf{W}), \quad (4)$$

where

$$\mathbf{W} = \begin{pmatrix} h \\ hu \end{pmatrix}, \quad \mathbf{F}(\mathbf{W}) = \begin{pmatrix} hu \\ hu^2 + \frac{1}{2}gh^2 \end{pmatrix},$$

$$\mathbf{Q}(\mathbf{W}) = \begin{pmatrix} 0 \\ -gh \frac{\partial B}{\partial x} \end{pmatrix}, \quad \mathbf{S}(\mathbf{W}) = \begin{pmatrix} 0 \\ -gM_b^2 \frac{u|u|}{h^{4/3}} \end{pmatrix}.$$

It is also well known that system (1) is strictly hyperbolic with real and distinct eigenvalues given as:

$$\lambda_1 = u - \sqrt{gh}, \quad \lambda_2 = u + \sqrt{gh}. \quad (5)$$

Notice that (1)-(3) have to be solved in a time interval and spatial domain equipped with given boundary conditions.

Numerical solution of the shallow water equation (1) has been subject of many research studies, and several numerical methods have been developed for their accurate and efficient solutions. In the current work, we consider four finite volume methods which have well established for many years as numerical solvers for hyperbolic systems of conservation laws. To deal with source terms in (1), we propose a splitting operator for which the differential source terms $\mathbf{Q}(\mathbf{W})$ and the non-differential source term $\mathbf{S}(\mathbf{W})$ are solved in two stages. Hence, we divide the time interval into subintervals $[t_n, t_{n+1}]$ with uniform size Δt and $t_n = n\Delta t$. We also use the notation $\mathbf{W}^n(x) = \mathbf{W}(x, t_n)$ to denote the discrete solution at time t_n . Thus, given the solution \mathbf{W}^n at time t_n , the solution \mathbf{W}^{n+1} at next time level, t_{n+1} is obtained using the following two-stage splitting procedure:

Step 1: Solve for $\widetilde{\mathbf{W}}$

$$\frac{\widetilde{\mathbf{W}} - \mathbf{W}^n}{\Delta t} + \frac{\partial \mathbf{F}(\mathbf{W}^n)}{\partial x} = \mathbf{Q}(\mathbf{W}^n). \quad (6)$$

Step 2: Solve for \mathbf{W}^{n+1}

$$\frac{\mathbf{W}^{n+1} - \widetilde{\mathbf{W}}}{\Delta t} = \mathbf{S}(\widetilde{\mathbf{W}}). \quad (7)$$

For the space discretization, we discretize the domain into control volumes $[x_{i-\frac{1}{2}}, x_{i+\frac{1}{2}}]$ with uniform length Δx for simplicity only. We use the notation \mathbf{W}_i^n to denote the space-averaged of $\mathbf{W} = \mathbf{W}(t, x)$ in the cell $[x_{i-\frac{1}{2}}, x_{i+\frac{1}{2}}]$ at time t_n , and $\mathbf{W}_{i+\frac{1}{2}}$ is the numerical flux at $x_{i+\frac{1}{2}}$ at time t as:

$$\mathbf{W}_i(t) = \frac{1}{\Delta x} \int_{x_{i-\frac{1}{2}}}^{x_{i+\frac{1}{2}}} \mathbf{W}(t, x) dx, \quad \mathbf{W}_{i+\frac{1}{2}} = \mathbf{W}\left(t, x_{i+\frac{1}{2}}\right).$$

Integrating the system (6) over the control domain $[x_{i-\frac{1}{2}}, x_{i+\frac{1}{2}}]$, one obtains the following fully discrete system:

$$\mathbf{W}_i^{n+1} = \mathbf{W}_i - \frac{\Delta t}{\Delta x} \left(\mathbf{F}_{i+\frac{1}{2}}^n - \mathbf{F}_{i-\frac{1}{2}}^n \right) + \Delta t \mathbf{Q}_i^n, \quad (8)$$

where $\mathbf{F}_{i\pm\frac{1}{2}}^n = \mathbf{F}(\mathbf{W}_{i\pm\frac{1}{2}}^n)$ are the numerical fluxes at $x = x_{i\pm\frac{1}{2}}$ and time $t = t_n$; whereas, \mathbf{Q}_i^n is a consistent discretization of the source term \mathbf{Q} in (6). Note that the spatial discretization (8) is complete when the numerical fluxes $\mathbf{F}_{i\pm\frac{1}{2}}$ and the source term \mathbf{Q}_i are reconstructed. Generally, this step can be carried out using any finite volume method developed in the literature for solving hyperbolic systems of conservation laws. In the present study, we consider the following finite volume reconstructions:

- Lax-Friedrich scheme [28]:

$$\mathbf{F}_{i+1/2}^n = \frac{1}{2} (\mathbf{F}(\mathbf{W}_{i+1}^n) + \mathbf{F}(\mathbf{W}_i^n)) + \frac{\Delta x}{2\Delta t} (\mathbf{W}_i^n - \mathbf{W}_{i+1}^n). \quad (9)$$

- Rusanov scheme [5]:

$$\mathbf{F}_{i+1/2}^n = \frac{1}{2} (\mathbf{F}(\mathbf{W}_{i+1}^n) + \mathbf{F}(\mathbf{W}_i^n)) + \frac{1}{2} \lambda (\mathbf{W}_i^n - \mathbf{W}_{i+1}^n), \quad (10)$$

where $\lambda = \max(\lambda_1^n, \lambda_2^n)$ is the Rusanov speed with λ_1 and λ_2 are the two eigenvalues associated with the system defined in (5).

- Roe scheme [21]:

$$\mathbf{F}_{i+1/2}^n = \frac{1}{2} (\mathbf{F}(\mathbf{W}_{i+1}^n) + \mathbf{F}(\mathbf{W}_i^n)) + \frac{1}{2} \mathbf{A}(\widehat{\mathbf{W}}_{i+1/2}^n) (\mathbf{W}_i^n - \mathbf{W}_{i+1}^n), \quad (11)$$

where $\widehat{\mathbf{W}}_{i+1/2}^n$ is the averaged state calculated as:

$$\widehat{\mathbf{W}}_{i+1/2}^n = \begin{pmatrix} \frac{h_i^n + h_{i+1}^n}{2} \\ \frac{\sqrt{h_i^n u_i^n} + \sqrt{h_{i+1}^n u_{i+1}^n}}{\sqrt{h_i^n + h_{i+1}^n}} \end{pmatrix}, \quad (12)$$

and \mathbf{A} is the Roe matrix defined as $\mathbf{A} = \mathbf{R}\mathbf{\Lambda}\mathbf{R}^{-1}$ with,

$$\mathbf{R} = \begin{pmatrix} 1 & 1 \\ \widehat{\lambda}_1 & \widehat{\lambda}_2 \end{pmatrix}, \quad \mathbf{\Lambda} = \begin{pmatrix} \widehat{\lambda}_1 & 0 \\ 0 & \widehat{\lambda}_2 \end{pmatrix},$$

where $\widehat{\lambda}_1$ and $\widehat{\lambda}_2$ are the two eigenvalues associated with the system defined in (5) evaluated at the Roe state (12).

- FVC scheme [4]: To reconstruct the numerical fluxes using the Finite Volume Characteristics (FVC) method, the shallow water equations (1) are first reformulated in an advective form as:

$$\begin{aligned} \frac{\partial h}{\partial t} + u \frac{\partial h}{\partial x} &= -h \frac{\partial u}{\partial x}, \\ \frac{\partial u}{\partial t} + u \frac{\partial u}{\partial x} &= -gh \frac{\partial}{\partial x} (h + B). \end{aligned} \quad (13)$$

Then, we use the method of characteristics to compute the solutions of (13) at the interfaces $x_{i\pm\frac{1}{2}}$. Thus, the associated characteristic curves $X_{i\pm\frac{1}{2}}(\tau)$ are computed

as solutions of the initial-value problem:

$$\begin{aligned} \frac{dX_{i\pm\frac{1}{2}}(\tau)}{d\tau} &= u(\tau, X_{i\pm\frac{1}{2}}(\tau)), \quad \tau \in [t_n, t_{n+1}], \\ X_{i\pm\frac{1}{2}}(t_{n+1}) &= x_{i\pm\frac{1}{2}}. \end{aligned} \quad (14)$$

To solve the ordinary differential equation (14), we use a second-order explicit Runge-Kutta method, see [4] for more details.

The numerical fluxes in the FVC scheme are obtained by integrating the advective equation (13) along the characteristics in the time interval $[t_n, t_n + \Delta t]$. Thus, assume an accurate approximation of the characteristics curves $X_{i\pm\frac{1}{2}}(t_n)$ is made, the intermediate solutions are obtained from (13) as:

$$\begin{aligned} h_{i+\frac{1}{2}}^n &= \widetilde{h}_{i+\frac{1}{2}}^n - \frac{\Delta t}{\Delta y} \widetilde{h}_{i+\frac{1}{2}}^n (u_{i+1}^n - u_i^n), \\ u_{i+\frac{1}{2}}^n &= \widetilde{u}_{i+\frac{1}{2}}^n - g \frac{\Delta t}{\Delta y} ((h^n + B)_{i+1} - (h^n + B)_i), \end{aligned} \quad (15)$$

where,

$$\widetilde{h}_{i+\frac{1}{2}}^n = h(t_n, X_{i+\frac{1}{2}}(t_n)), \quad \widetilde{u}_{i+\frac{1}{2}}^n = u(t_n, X_{i+\frac{1}{2}}(t_n)),$$

are solutions at the departure points $X_{i\pm\frac{1}{2}}(t_n)$ computed by a cubic Lagrange interpolation from the gridpoints of the control volume where the departure point $X_{i\pm\frac{1}{2}}(t_n)$ belongs. Hence, the numerical fluxes for the FVC scheme are defined by:

$$\mathbf{F}_{i+1/2}^n = \begin{pmatrix} h_{i+\frac{1}{2}}^n u_{i+\frac{1}{2}}^n \\ h_{i+\frac{1}{2}}^n (u_{i+\frac{1}{2}}^n)^2 + \frac{1}{2} g (h_{i+\frac{1}{2}}^n)^2 \end{pmatrix}, \quad (16)$$

where $h_{i+\frac{1}{2}}^n$ and $u_{i+\frac{1}{2}}^n$ are intermediate solutions approximated in (15).

For the approximation of the source term in (8), we use the well-balanced discretization of the source term \mathbf{Q}_i as:

$$gh \frac{\partial Z}{\partial x} \approx g \frac{h_{i+1} + 2h_i + h_{i-1}}{4} \frac{Z_{i+1} - Z_{i-1}}{2\Delta x}. \quad (17)$$

Note that, using this discretization of the source term, the scheme (8) satisfies the well-known C-property [4]. It should be stressed that other numerical solvers for the shallow water equation (1) can also be used in the present study without major conceptual modifications.

III. OPTIMAL CONTROL METHOD FOR RECONSTRUCTION OF TOPOGRAPHY

In this section, we present numerical tools used for the optimal control reconstruction of topography in dam-break flows. In general, Data Assimilation (DA) aims at combining field observations with different model inputs in order to reduce the uncertainty of a numerical model and improve its predictability in an optimal manner, see [16] among others. For hydraulics, a numerical model relies on mathematical description of the dynamic whereas, observation produces more accurate description of the actual state of the flow.

Despite producing different outputs, the resulting uncertainty produced by the DA is below the uncertainties of both the numerical model and the observational data. Although the DA has been initially used for weather forecasting, different research topics have adopted this tool for operational purposes. In hydraulics, the DA is still emerging compared to other geophysical fields, see for example [17], [2] and further references therein. Technically, the DA aims at controlling the value of the model parametrization responsible for the largest amount of uncertainty. The optimality of this control is achieved due to the information given by the observations. Here, the cost function can be formulated as:

$$J(x) = \frac{1}{2} \|x - x_B\|_{\mathbf{B}} + \frac{1}{2} \|y - \mathcal{H}(x_B)\|_{\mathbf{O}}, \quad (18)$$

where x_b is a prior knowledge (initial guess) of the parameter, which is usually referred to as the background, y the observation, and \mathcal{H} the observation operator. Since the DA takes into account the uncertainties, both norms $\|\cdot\|_{\mathbf{B}}$ and $\|\cdot\|_{\mathbf{O}}$ are defined within the uncertainty region of the background and the observation, respectively. It should also be noted that the observation is not necessarily of the same nature as the parameter x , and for example, we may correct the bathymetry using observations of the water level. In this case, the observation operator reduces to a linear interpolation operator. However, in most cases of hydraulic applications, this operator is highly nonlinear.

The main objective of the DA is to minimize the cost function $J(x)$ under the constraints given by the uncertainties on the observation and the background. In general, (18) does not have an exact solution. However, a statistical estimation of the optimal parameter that minimizes the function $J(x)$ can be achieved using some inference methods such as filtering. When the uncertainties expressed around the parameter and the observation are supposed to follow a Gaussian probability distribution, the filtering could be carried out using the Kalman filter, compare [24].

A. Ensemble Kalman Filter

For the assumption of Gaussian uncertainties, estimating the probability distribution reduces to evaluating the mean and the covariance matrices. Thus, optimizing the functional (18) yields to find the main parameter x and its covariance matrix. In this framework, the background and the observation are fully defined by their covariance matrices \mathbf{B} and \mathbf{O} , respectively. The Kalman Filter (KF) is a sequential DA algorithm which is able to reproduce these solutions under the assumption given above. This means that the KF provides a new optimal solution for (18) whenever an observation is available. For this reason, this algorithm is classically divided into two steps: (i) the forecast stage and (ii) the analysis stage. During the first one, the model is dynamically moving forward in time with the background information until an observation is available. The analysis stage is then achieved by correcting the value of the background such that,

$$x_a = x_b + \mathbf{K}(y - \mathbf{H}x), \quad (19)$$

where x_a is the analyzed value (the corrected value) of the parameter and \mathbf{K} is the so-called Kalman gain matrix and is defined by:

$$\mathbf{K} = \mathbf{B}\mathbf{H}^T (\mathbf{H}\mathbf{B}\mathbf{H}^T + \mathbf{O})^{-1}. \quad (20)$$

As mentioned before, the KF is not only able to give the mean value but also the uncertainties modeled here in its covariance matrix:

$$\mathbf{A} = (\mathbb{I} - \mathbf{K}\mathbf{H})\mathbf{B}, \quad (21)$$

where \mathbb{I} is the identity matrix. Note that, in most hydraulic applications, the governing equations describing the physics are highly nonlinear such as the shallow water equation (1). Consequently, the KF is of no use because the operator \mathcal{H} is not linear. One interesting way to overcome this drawback is to use the Ensemble Kalman Filter (EnKF).

In practice, the EnKF relies on the stochastic approach in order to overcome the problem of nonlinearity in the classical KF, see for instance [7]. Here, instead of considering the whole distribution for modeling the uncertainty of the parameter under study, one uses a set of sample $x_B = (x_b^{(1)}, \dots, x_b^{(N)})$ based on the distribution (Ensemble). Indeed, using Monte-Carlo simulations of the model, it is possible to stochastically estimate the different matrices forming the Kalman gain matrix such that,

$$\mathbf{B} = \frac{1}{N-1} (x_b - \bar{x}_b)(x_b - \bar{x}_b)^T, \quad (22)$$

where \bar{x}_b denotes the mean value of x_b . Therefore, the covariance functions can be approximated using statistical averages of the solution ensemble.

B. Twin Experiment

In the present study, we use a twin experiment to assess the quality of the DA algorithm. This is a well-known methodology used when access to real data is not possible, see [26] among others. The experiment consists of using a simulation with a supposed true value of the bathymetry. The hydraulic state resulting from this simulation will be used as the observation. Then, using another value of the bathymetry (referred to by the background), the EnKF will be applied. The analysis obtained by the proposed algorithm will be compared to the bathymetry which allows to obtain the hydraulic state of the observation. The EnKF is based on a stochastic approach such that the background value of the bathymetry will be perturbed. Hence, using an ensemble of bathymetric fields, a set of hydraulic state can be obtained. It is worth mentioning that the perturbation in this case follows a normal law with a mean value set to the background value and a fixed coefficient of variation. In order to have a good estimation of the reconstruction, the algorithm is performed several times. The iteration procedure is used here and for each test example we will mention the number of loops used. In summary, the proposed algorithm can be carried out using the following steps:

- 1) Perform a first simulation in order to generate the observation data.

- 2) Generate a set of bathymetric fields around the background value.
- 3) Run the ensemble of simulation.
- 4) Compute the Kalman Filter gain using a stochastic step as:

$$\begin{aligned}\mathbf{B}\mathbf{H}^\top &= \frac{1}{N} (B - \bar{B}) (h - \bar{h})^\top, \\ \mathbf{H}\mathbf{B}\mathbf{H}^\top &= \frac{1}{N} (h - \bar{h}) (h - \bar{h})^\top.\end{aligned}$$

- 5) Compute the analysis state.
- 6) If the number of iterations is not achieved redo steps 2), 3) and 4).

In all our simulations, the coefficient of variation is set to 20% unless stated otherwise. Furthermore, the Root Mean Square (RMS) error is used to quantify the accuracy and performance of the proposed algorithm.

IV. NUMERICAL RESULTS

In this section, we present numerical results for a dam-break problem over a non-flat bed. The main goals of this test example are to illustrate the numerical performance of the techniques described above and to verify numerically their capability to reconstruct the correct topography using different initial guesses. Here, we solve the system (1)-(3) in a 30 m long channel with the upstream and downstream water heights $h_l = 1$ m and $h_r = 0.5$ m, respectively. The dam is located at $x_0 = 15$ m, the gravitational acceleration $g = 9.81 \text{ m/s}^2$, the Manning coefficient $M_b = 0.03 \text{ s/m}^{1/3}$ and the computational domain is discretized into 100 control volumes with $\Delta x = 0.3$ m. In all the computations reported herein, the Courant number is set to $Cr = 0.75$ and the time stepsize Δt is adjusted at each time step according to the Courant-Friedrichs-Lewy condition:

$$\Delta t = Cr \frac{\Delta x}{\max(|\lambda_1^n|, |\lambda_2^n|)}, \quad (23)$$

where λ_1 and λ_2 are the eigenvalues given by (5). We first solve the forward problem for a total time of $t = 2$ s over a known bed defined by a hump as:

$$B(x) = \frac{1}{5} \exp\left(-\frac{(x-14)^2}{20}\right),$$

and store the water height as given locations to be used later as observational data in the Twin experiment. We examine the performance of the proposed method by changing (i) initial bed guesses, (ii) number and locations of observations, and (iii) finite volume schemes solving the shallow water equations.

A. Sensitivity on Background Values

We first examine the effects of the initial guess used for the bed function (background) on the accuracy of the reconstructed bed (analysis). The purpose here is to identify the ability of the EnKF to reconstruct the bathymetric field using different values for the background. In this example,

TABLE I
RMS ERRORS FOR THE BED RECONSTRUCTION USING DIFFERENT INITIAL BED FUNCTIONS

| Bed function | RMS error |
|--------------|-----------|
| $B_1(x)$ | 0.008075 |
| $B_2(x)$ | 0.009475 |
| $B_3(x)$ | 0.03158 |
| $B_4(x)$ | 0.07210 |

the following functions are implemented for the background bathymetry:

$$\begin{aligned}B_1(x) &= 0, \\ B_2(x) &= \frac{1}{10} \exp\left(-\frac{(x-10)^2}{20}\right), \\ B_3(x) &= \frac{1}{5}, \\ B_4(x) &= \frac{1}{5} \exp\left(-\frac{(x-5)^2}{10}\right) + \frac{1}{5} \exp\left(-\frac{(x-25)^2}{10}\right).\end{aligned} \quad (24)$$

The EnKF algorithm is run for each of background value defined in (24) using an Ensemble size of 200 simulations. Here, as numerical solver for the direct problem, we use the Roe scheme. The obtained numerical results for the expected bed are shown in Fig. 1. We also include in this figure the observational data, the initial guess and the target bed for each run. As expected for a dam-break problem, at time $t = 0$, the dam collapses and the flow problem consists of a shock wave traveling downstream and a rarefaction wave traveling upstream. These features are well captured by our method in the results shown in Fig. 1. In order to assess the quality of the DA algorithm for each of background used, the RMS error is computed for each experiment. Table I represents the value of the RMS error for the four bed functions in (24).

It is clear from the results shown in Fig. 1 and Table I that the bed reconstruction is impacted by the value of the background used in the simulations. Indeed, using $B_1(x)$ and $B_2(x)$ as background values in the optimal control method produces better results than those obtained using $B_3(x)$ and $B_4(x)$. This is mainly due to the fact that the selected background values $B_1(x)$ and $B_2(x)$ are close to the target bed. As suggested by the value of RMS error, the correction gained one order of magnitude just by getting as close as possible to the target solution. It should be pointed out that this is one of the major difficulties when dealing with DA to reconstruct the bathymetry in hydraulics. This problem has also been reported in other studies, see for example [19]. This confirms that numerical tools can not replace *in-situ* experiments, and field works carried out by hydraulic engineers remains an essential stage for bed reconstructions. In fact, using field measurements, the background value used for the bathymetry can be very close to the target bed which would help DA algorithms to gain accuracy. The proposed method performs well for this test example and the target bed can be accurately reconstructed without requiring complicated

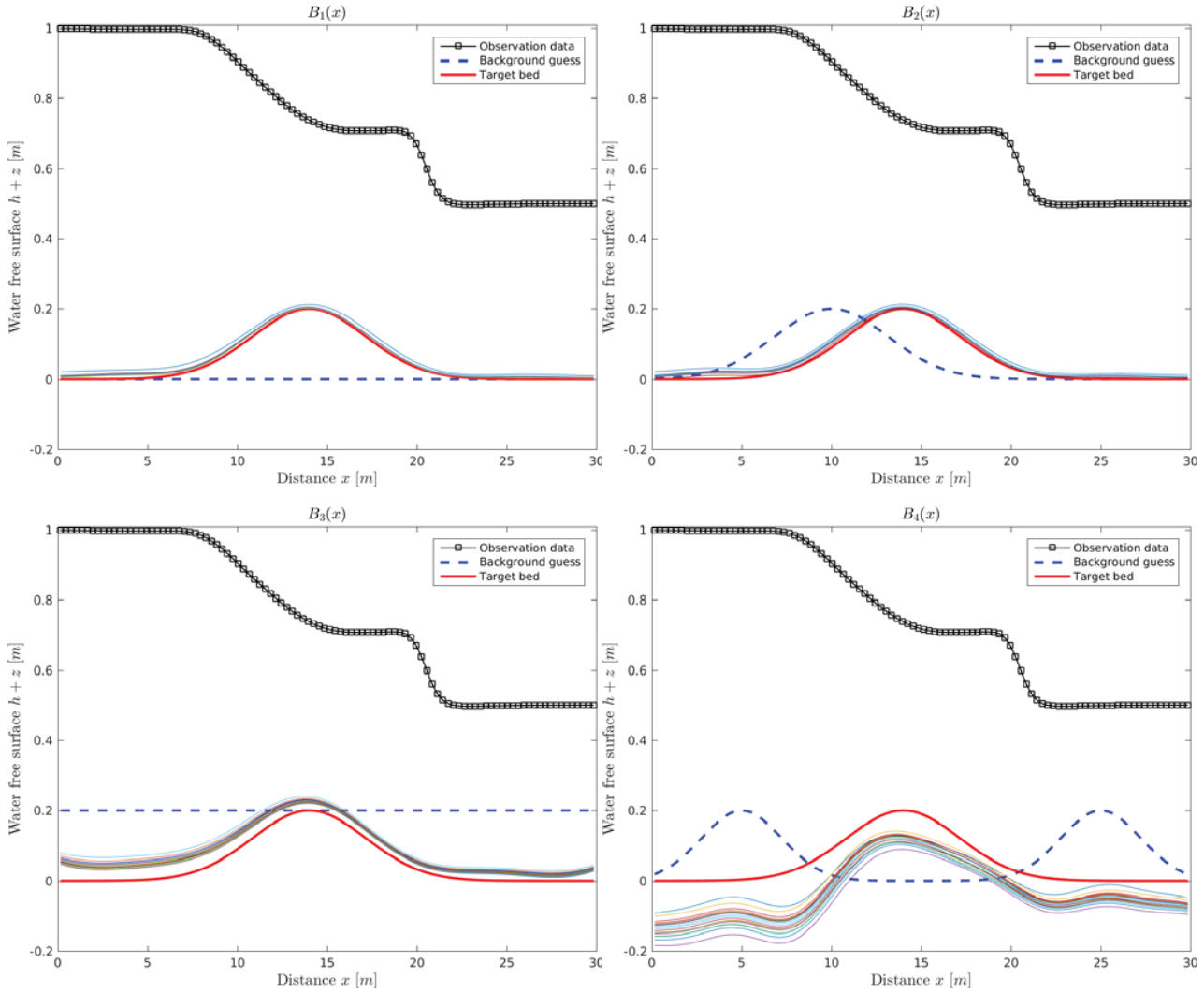


Fig. 1 Results for the bed reconstruction using different initial bed functions.

tools.

B. Sensitivity on Finite Volume Schemes

In addition to the background value used in the method, selection of the numerical scheme for shallow water equations constitutes an important key in DA algorithms. It is therefore important to assess the ability of such tools to correctly reconstruct the bathymetric field. Generally, there are two main key parameters that should be kept in mind when using a model with a stochastic-based algorithm like the EnKF namely, the choice of the numerical model and the uncertainty propagation in this model. In this section, we evaluate the impact of these two proprieties on the bathymetry reconstruction. We assess the impact of the four finite volume schemes considered in this study on the reconstruction of topography in dam-break flows. We consider the same parameters as in the previous run and solve the forward problem Lax-Friedrichs, Rusanov, Roe, and FVC scheme at

final time of $t = 2$ s. A set of 100 observations of the water height uniformly distributed in the computational domain is used for the bed reconstruction. As an initial guess for the bed, we use the background value $B_2(x)$ defined in (24). In our simulations for this run, 100 samples and 20 iterations are used in the EnKF algorithm.

In Fig. 2, we present the obtained results for bed reconstruction using the four considered finite volume schemes. The evolution of RMS errors for these schemes at each iteration is illustrated in Fig. 3. The results reveal that the EnKF does not show the same trends for these finite volume schemes. Indeed, the EnKF is based on a stochastic method such that the uncertainty is propagated into the model and the matrix which constitutes the Kalman Gain Matrix will be different depending on the numerical method used. The results shown in Fig. 3 for the RMS errors confirm that the Roe and FVC schemes are more consistent than the Lax-Friedrich and Rusanov schemes. The numerical diffusion generated

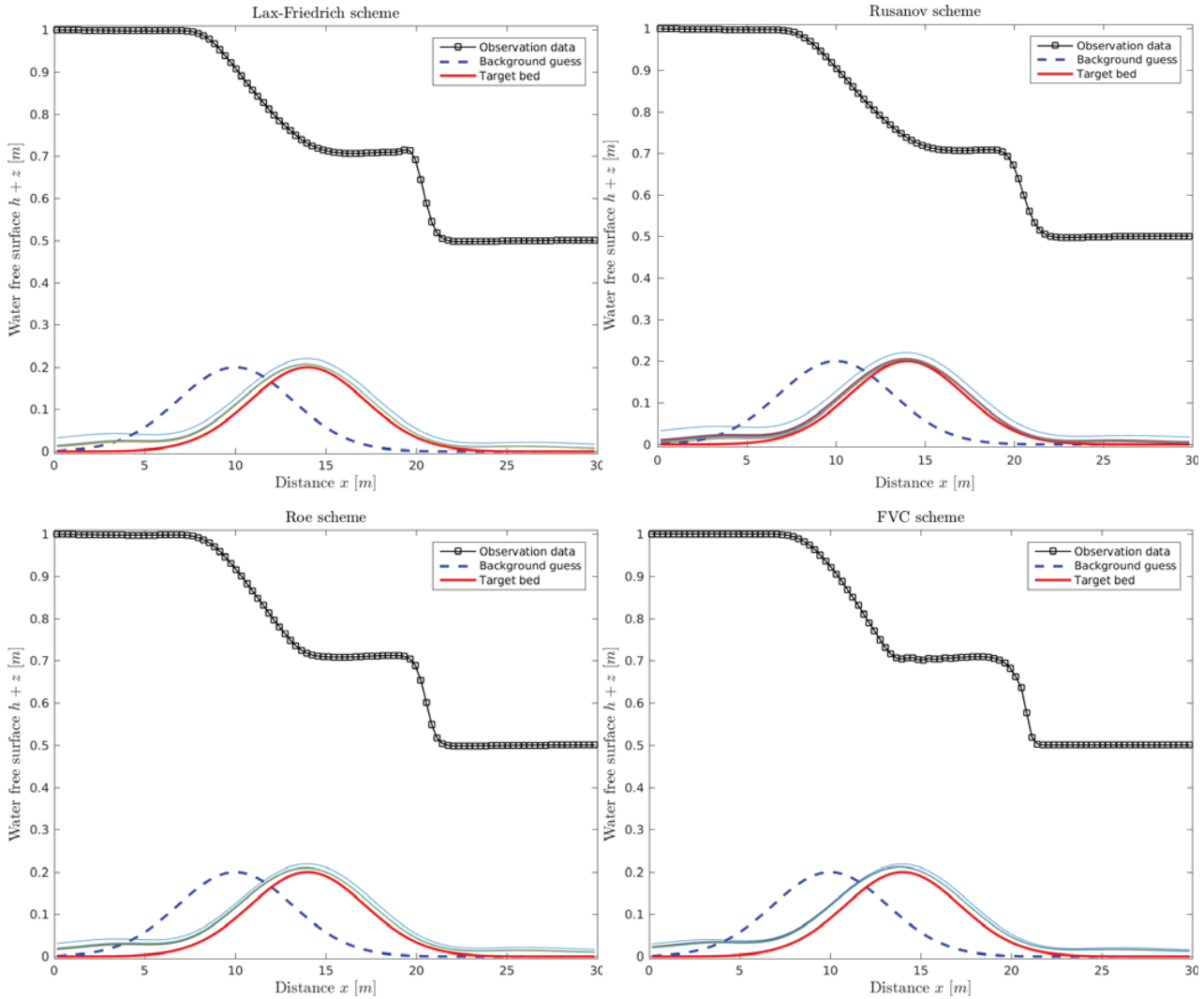


Fig. 2 Results for the bed reconstruction using different fine volume schemes

by Lax-Friedrich and Rusanov schemes could explain these differences whereas, the Roe and FVC schemes have proven to be very flexible to catch strong nonlinearity and discontinuities in the shallow water equations. Note that the main advantage of high accurate volume schemes lies in the fact that they can converge easily when used in algorithms like EnKF. However, the associated uncertainties may increase in the simulations which leads to poor reconstruction in the DA algorithm. On the other hand, using low accurate schemes, the numerical dissipation makes the DA algorithm very hard to converge, but they could easily lead to satisfying corrections.

C. Sensitivity on Uncertainty in the Background Value

Next, we check the impact of the uncertainty on the background and its effect on the bed reconstruction. In this test, we run the EnKF algorithm using three different uncertainty assumption on the bed. It should be stressed

that the well-established numerical methods for shallow water flows have been considered only the deterministic problems. The solutions are then admitted without paying attention to the uncertainty that are ubiquitous to any numerical model. Note that the classical way to assess the uncertainty of a numerical model is to reconsider it as a stochastic input. This means that the model parameters, boundary and initial conditions have to be seen as random parameters and/or processes. In this run, we consider the same parameters and flow conditions as in the previous case but we introduce an uncertainty in the bed. Three different levels of uncertainty are applied in this test with the coefficient of variation in the bed $CV_b = 7\%$, 11% and 16% .

In Fig. 4, we present the results obtained using the considered levels of uncertainty and Fig. 5 depicts the RMS errors associated with these levels. As it can be seen in these figures, increasing the value of the background uncertainty may help to achieve a good level of correction. In fact, when

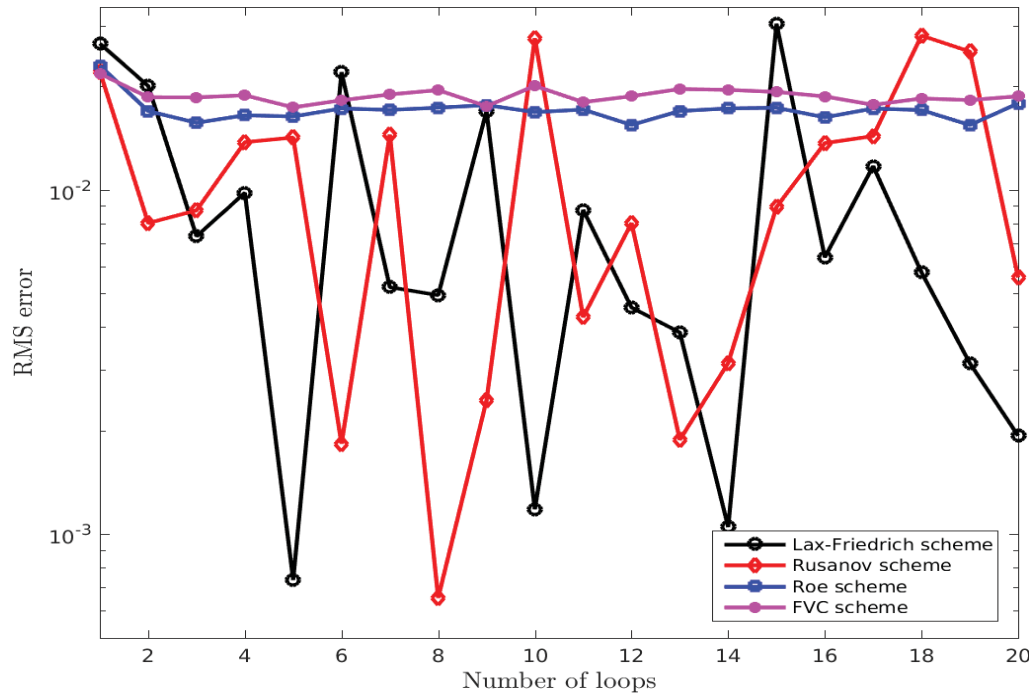


Fig. 3 RMS errors for the bed reconstruction using different fine volume schemes

using a Bayes theorem-based algorithm, one should keep in mind that the distribution of the parameters to be inferred has to be large enough in order to contain the uncertainty of the observation. This problem has been discussed in the literature, see [14] among others.

The correction obtained using the EnKF correction could highly be improved by applying the algorithm iteratively several times. As consequence, the quality of the reconstructed bed is impacted by the number of iterations used. In Table II, we demonstrate the effect of changing the number of iterations at two different times $t = 1$ s and $t = 2$ s. Clearly, the DA is impacted by the assimilation window that the quality of the correction with the DA depends on the physical time used in the simulations. Results included in Table II give a clear idea on the impact of these two parameters on the correction of the bathymetry in dam-break flows.

As observed in the obtained results, the quality of the reconstruction does not improve with iterations when using an assimilation window at time $t = 1$ s. This is due to the fact that the hydraulic has not been developed enough and all the information is still locked. Note that, this is an expected result if the well-known Best Linear Unbiased Estimator (BLUE) is employed. However, for the assimilation window at time $t = 2$ s, the quality of the bed reconstruction improves considerably with the number of iterations. Moreover, the quality of the bed reconstruction is improved in this case compared to the first case at $t = 1$ s. Thus, these results emphasize the importance of considering a time-based algorithm such as the EnKF rather than a time-independent one such as the BLUE.

TABLE II
EVOLUTION OF RMS ERRORS FOR THE BED RECONSTRUCTION USING DIFFERENT UNCERTAINTIES IN THE BACKGROUND VALUE FOR DIFFERENT NUMBER OF LOOPS AT TIME $t = 1$ s AND $t = 2$ s.

| Number of iteration | RMS error | |
|---------------------|-----------|-----------|
| | $t = 1$ s | $t = 2$ s |
| 5 | 0.0382 | 0.01274 |
| 10 | 0.03391 | 0.01014 |
| 15 | 0.03601 | 0.009825 |
| 20 | 0.03666 | 0.009815 |
| 25 | 0.03754 | 0.009737 |
| 30 | 0.03733 | 0.009459 |
| 35 | 0.03764 | 0.009001 |
| 40 | 0.03724 | 0.009263 |
| 45 | 0.03693 | 0.008525 |
| 50 | 0.03654 | 0.009812 |

It is also evident from the presented results that the assimilation is closely linked to the hydrodynamic. Hence, using the stochastic approach, one should make sure that the hydrodynamic has been developed enough to ensure a better correction. However, it is important to point out that the simulation time will also impact the uncertainty propagation in the numerical model used in the simulations. Therefore, there is a clear trade-off related to simulation time versus the uncertainty that should be kept under consideration when

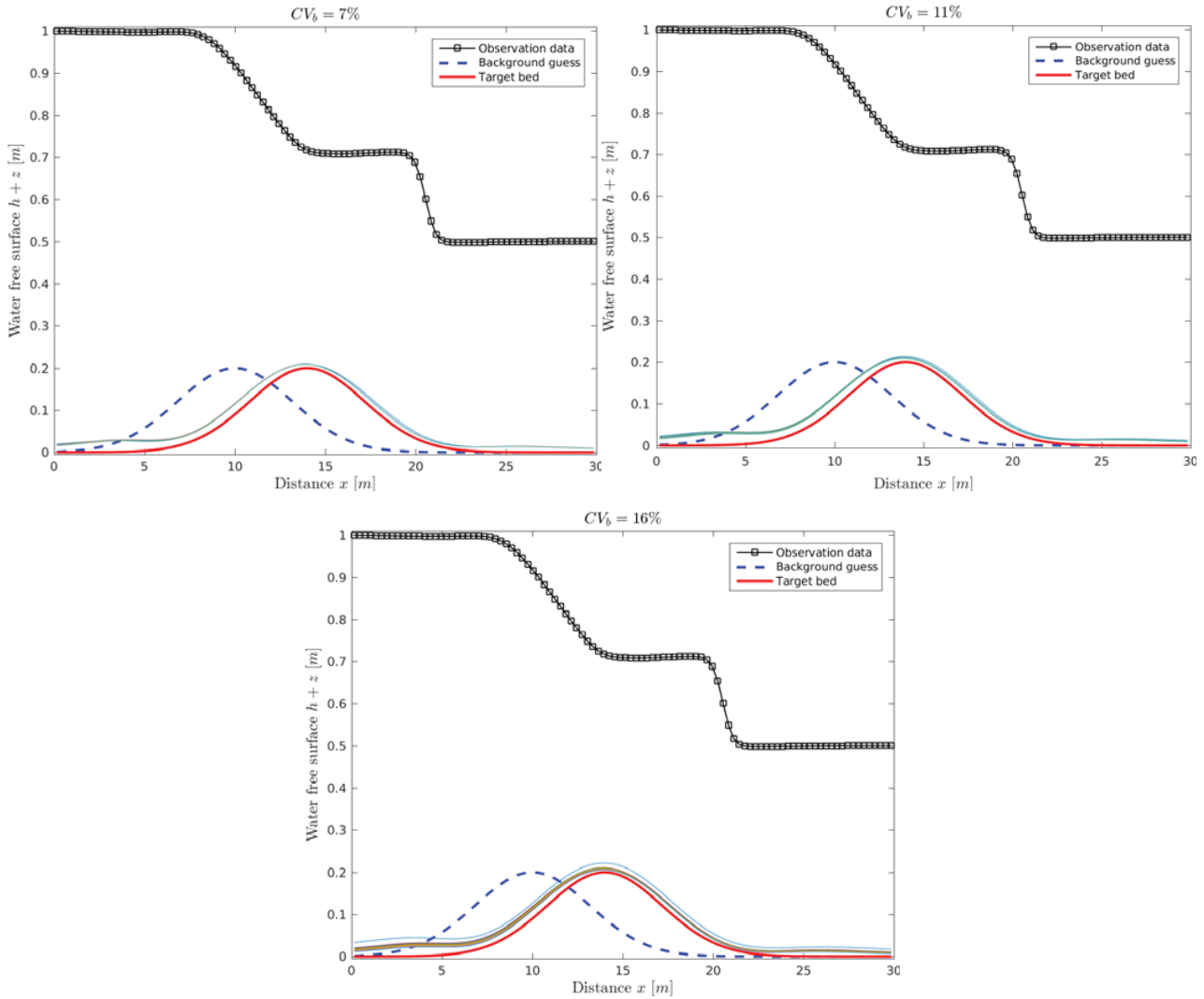


Fig. 4 Results for the bed reconstruction using different uncertainties in the background value

using the DA for hydrodynamic models. The best use of such algorithms dictates that the one should have a good length of assimilation window while paying attention to the uncertainty.

D. Sensitivity on Observed Data at the Free Surface

Observed data is considered to be one of the most important keys in DA algorithms. Using the Twin experiment, it allows to assess the impact of the key factor on the quality of bed corrections. The level of discrepancy in these data will have a direct effect on the quality of the algorithms. Thus, in order to accurately predict the bathymetry in dam-break flows, DA algorithms should be precise and accurate with respect to the observation setting. For this purpose, a dam-break problem with the same flow conditions as in the previous test is used in this run. In this section, three main parameters are investigated with regards to the observation data: (i) the number of the observation data, (ii) the location of the observation data and (iii) the uncertainty in the observation data.

First, we assess effects of the number of observation data used in the EnKF. This is especially important in the case where one needs to correct a space-based parameter such as the bathymetry. In this test case, different numbers of observations are used for the bed reconstruction and the obtained RMS errors for each number are presented in Table III. It is clear that, as the number of iterations increases the accuracy of the reconstructed bed increases and the root mean square error decreases accordingly. However, given the hydrodynamic of the dam-break under study, location of the observation data is important. This is, for example, what explains the difference between the run using 50 observations and the run using 25 observations. Note that the effects of the number of observation data is clearly seen on the correction in a way that as more sets of observation data are available, the better the correction is. From a practical point of view, this would mean that one needs to install gauges along the whole flow channel

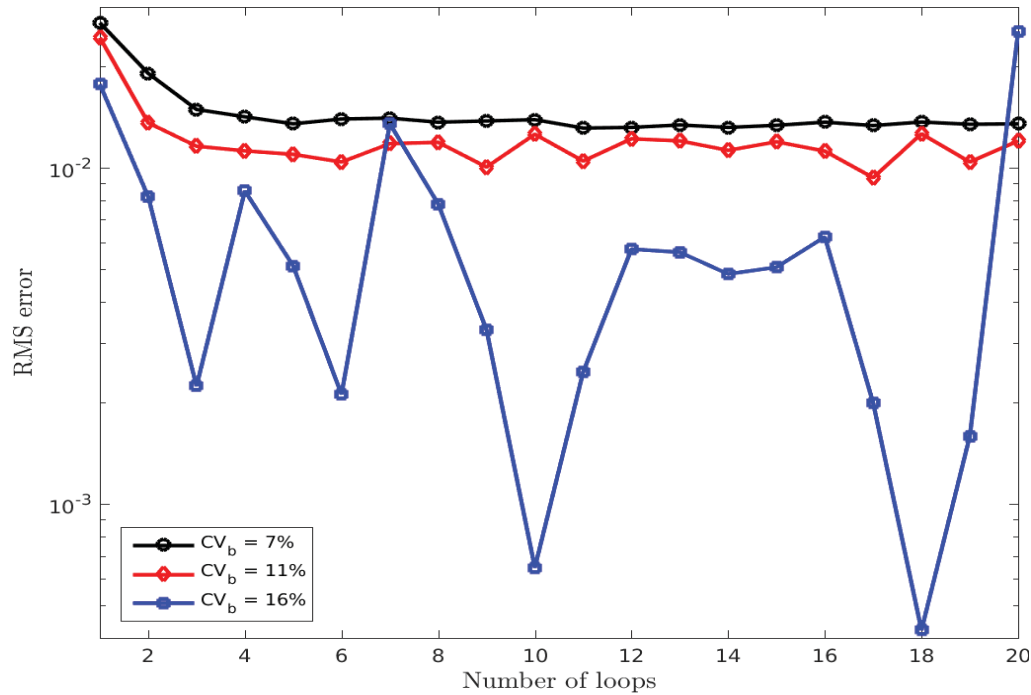


Fig. 5 RMS errors for the bed reconstruction using different uncertainties in the background value

to collect measurements, which is less likely to be feasible from an economic perspective. An alternative way would be through the use of remote sensing data. However, the limitation in these techniques is associated with the uncertainty in the recorded measurements. Next, we examine the effects of the location of observation data and the uncertainty on these data.

TABLE III
RMS ERRORS FOR THE BED RECONSTRUCTION USING DIFFERENT
NUMBER OF THE OBSERVATION DATA

| Observations | RMS error |
|--------------|-----------|
| 5 | 0.06957 |
| 10 | 0.01604 |
| 20 | 0.009025 |
| 25 | 0.00739 |
| 50 | 0.031127 |
| 100 | 0.009344 |

To examine the effect of the spatial distribution of the observed data on the bed reconstruction, we run the same example as before but change the location of these data. Here, three different locations of the observation are tested along the flow channel in both downstream and upstream. More precisely, we select observation data in the upstream region between 1 *m* and 10 *m*, in the middle region between 11 *m* and 20 *m*, and in the downstream region between 21 *m* and 30 *m*. The obtained results are illustrated in Fig.

TABLE IV
RMS ERRORS FOR THE BED RECONSTRUCTION USING DIFFERENT
LOCATIONS OF THE OBSERVATION DATA

| Location range | RMS error |
|---------------------------|-----------|
| 1 <i>m</i> - 10 <i>m</i> | 0.1038 |
| 10 <i>m</i> - 20 <i>m</i> | 0.0062 |
| 20 <i>m</i> - 30 <i>m</i> | 0.0814 |

6 and the associated RMS errors are summarized in Table IV. Under the considered flow conditions, these results clearly highlight the importance of the location in observations for the correction. Again, the correction is highly dependent on the hydrodynamic, as previously mentioned. It is also evident that, when the dam break occurs, the dynamics are mostly concentrated around the dam location. This is mainly the reason why the best bed reconstruction is obtained when the observation are around the dam location. Furthermore, when the observation data are located downstream, the EnKF produces a better correction. Needless to say that, dealing with shallow water equations, the waves that propagates downstream and upstream do not have the same velocity. It is expected that the waves propagating downstream have more speed than the upstream ones. This explains the reason why the correction happening downstream is better than the upstream correction.

Finally, we assess the sensitivity of the EnKF on the inherited uncertainty in the observation data. This is an important feature that should be taken under consideration

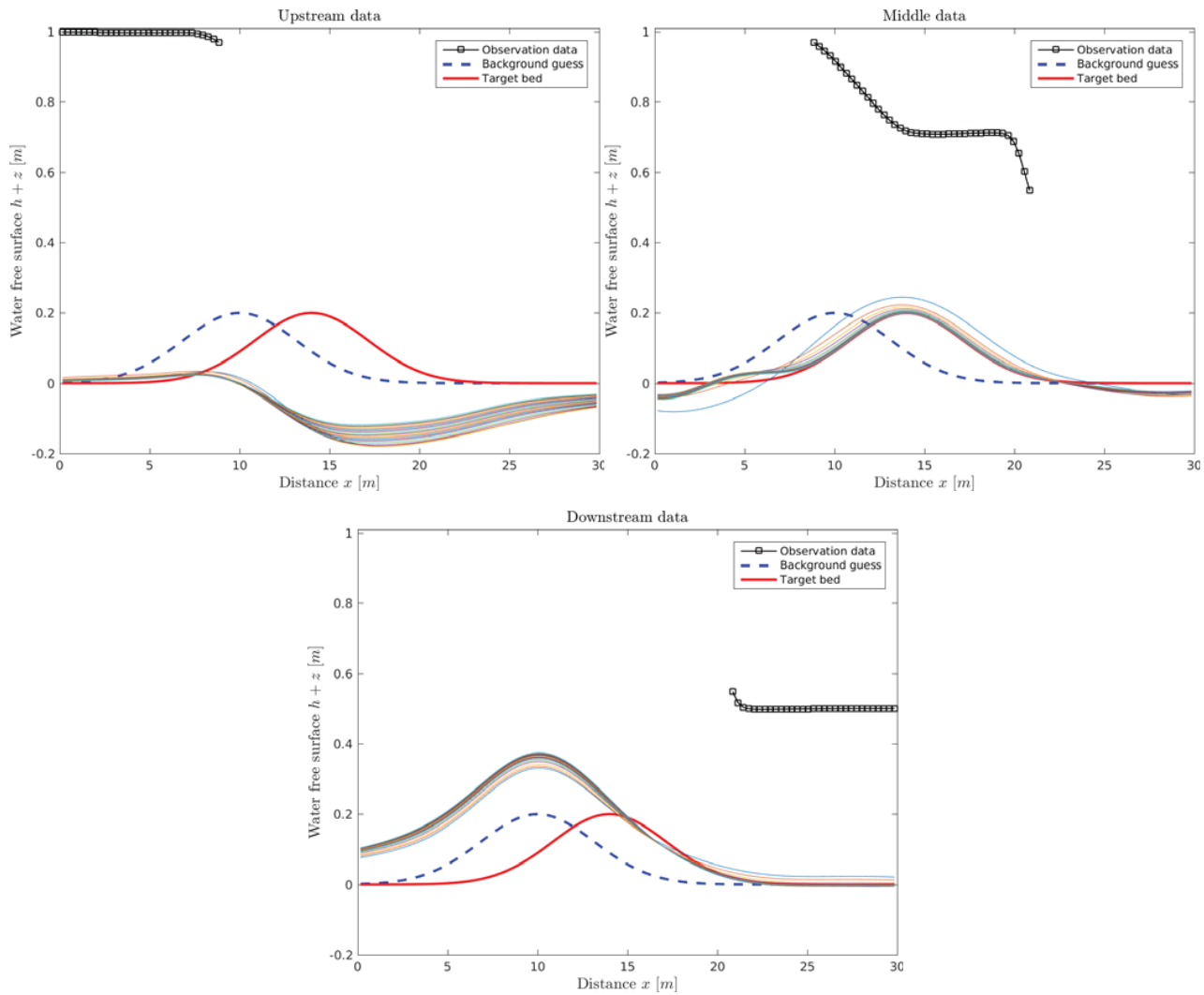


Fig. 6 Results for the bed reconstruction using different locations of the observation data

TABLE V
RMS ERRORS FOR THE BED RECONSTRUCTION USING DIFFERENT
UNCERTAINTY IN THE OBSERVED DATA

| Coefficient of variation | RMS error |
|--------------------------|-----------|
| 0.05 | 0.07234 |
| 0.10 | 0.06092 |
| 0.15 | 0.04825 |
| 0.20 | 0.06646 |
| 0.25 | 0.03605 |
| 0.30 | 0.009845 |

when dealing with reconstruction of a hydraulic field using the DA. In practice, different kind of observation would produce different measurements and each measurement is always accompanied with a range of uncertainty. In our computations

reported here, we consider six different uncertainty values with coefficient of variations $CV_b = 5\%$, $CV_b = 10\%$, $CV_b = 15\%$, $CV_b = 20\%$, $CV_b = 25\%$ and $CV_b = 30\%$. We also use the same flow condition as those used in the previous test cases.

In Fig. 7, we present the obtained results for this run and the associated RMS errors are included in Table V for the considered coefficient of variations. As can be seen, the uncertainty on the observation data greatly impacts the correction and it can lead to big discrepancies in the required results. It is also clear from the RMS errors in Table V that, increasing the uncertainty in the observation data results in an increase in the RMS error. It is worth to mention that the DA is a trade off between the background values and the observation data used for the bed reconstruction. The quantity and quality of the background values and the observation data highly influence the algorithm outcome. Consequently, if the uncertainty of the observation data increases, one would expect more confidence on the background values. This

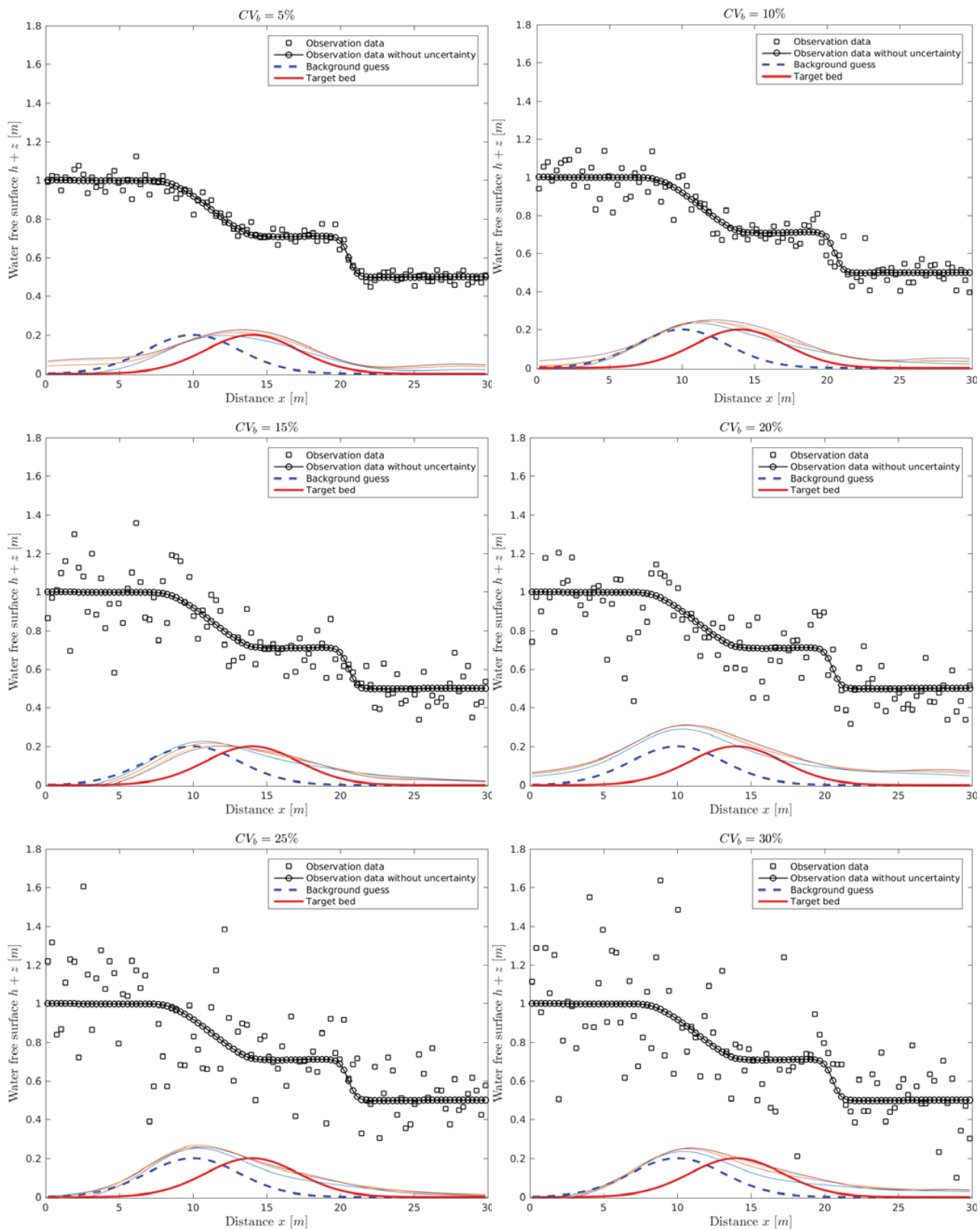


Fig. 7 Results for the bed reconstruction using different uncertainty in the observed data.

fact is supported by the results presented in Fig. 7, as the reconstruction hardly moves from the background value.

V. CONCLUSION

We have proposed a robust optimal control method for the bed reconstruction in dam-break flow problems. The governing equations consist of the nonlinear system of shallow water equations with bathymetric effects. As numerical solvers for the direct simulations, we have considered a class of four finite volume schemes. The optimal control methodology is based on the Ensemble Kalman Filter for the bed reconstruction. The performance of the proposed method is examined using different numbers and locations of the observed data, different number of loops, and different initial guesses for the bed topography. We have also added stochasticity to the initial guess for the bed as well as the observed data. In all cases, the method accurately captures the expected bed confirming its ability to reconstruct the bed topography from noisy observational data. In addition, the computational results obtained for the considered test cases demonstrate the accuracy and efficiency of the proposed method. The presented results also reveal good shock resolution with high accuracy in smooth regions and without any spurious oscillations near the shock areas. Although we have restricted our simulations to one-dimensional problems, the optimal control method investigated in the current work can be extended to free-surface flows in two space dimensions with viscous terms, Coriolis forces and over complex topography. These and further issues are the subject of future investigations.

REFERENCES

- [1] H. Abida. Identification of compound channel flow parameters. *Journal of Hydrology and Hydromechanics*, 57:172–181, 2009.
- [2] S. Barthélémy, S. Ricci, O. Pannekoucke, O. Thual, and P. Malaterre. Emulation of an Ensemble Kalman Filter algorithm on a flood wave propagation model. *Hydrology and Earth System Sciences Discussions*, 10:6963–7001, 2013.
- [3] F. Benkhaldoun, S. Sari, and M. Seaid. A flux-limiter method for dam-break flows over erodible sediment beds. *Applied Mathematical Modelling*, 36(10):4847–4861, 2012.
- [4] F. Benkhaldoun and M. Seaid. A simple finite volume method for the shallow water equations. *J. Comp. Applied Math*, 234:58–72, 2010.
- [5] F. Bouchut. *Nonlinear Stability of Finite Volume Methods for Hyperbolic Conservation Laws and Well-Balanced Schemes for Sources*. Birkhäuser, Basel, 2004.
- [6] W. Cheng and G. Liu. Analysis of non-linear channel friction inverse problem. *Frontiers of Architecture and Civil engineering in China*, 2:205–210, 2007.
- [7] G. Evensen. The Ensemble Kalman Filter: Theoretical formulation and practical implementation. *Ocean Dynamics*, 53(4):343–367, 2003.
- [8] M. Le Gal, D. Violeau, R. Ata, and X. Wang. Shallow water numerical models for the 1947 gisborne and 2011 tohoku-oki tsunamis with kinematic seismic generation. *Coastal Engineering*, 139:1–15, 2018.
- [9] P. Garcia-Navarro, A. Frás, and I. Villanueva. Dam-break flow simulation: some results for one-dimensional models of real cases. *Journal of Hydrology*, 216(3-4):227–247, 1999.
- [10] C. Heining and N. Askel. Bottom reconstruction in thin-film flow over topography: Steady solution and linear stability. *Physics and Fluids*, 21:321–331, 2009.
- [11] R. Hildale and D. Raff. Assessing the ability of airborne liDAR to map river bathymetry. *Earth Surf.Process*, 33:773–783, 2008.
- [12] A. Humberto, E. Schubert, and F. Sanders. Two-dimensional, high-resolution modeling of urban dam-break flooding: A case study of baldwin hills, california. *Advances in Water Resources*, 32(8):1323–1335, 2009.
- [13] E. LeMeur, O. Gagliardini, T. Zwinger, and J. Ruokolainen. Glacier flow modelling: A comparison of the shallow ice approximation and the full-stokes solution. *Comptes Rendus Physique*, 5:709–722, 2004.
- [14] F. Lu, M. Morzfeld, X. Tu, and A. Chorin. Limitations of Polynomial Chaos Expansions in the bayesian solution of inverse problems. *Journal of Computational Physics*, 282:138–147, 2015.
- [15] S. Martínez-Aranda, J. Murillo, and P. García-Navarro. A 1d numerical model for the simulation of unsteady and highly erosive flows in rivers. *Computers & Fluids*, 181:8–34, 2019.
- [16] G. Michael and P. Malanotte-Rizzoli. Data Assimilation in metrology and oceanography. *Advances in Geophysics*, 33:141–266, 1991.
- [17] N. El Moçayd. *La décomposition en polynôme du chaos pour l'amélioration de l'assimilation de données ensembliste en hydraulique fluviale*. PhD thesis, 2017.
- [18] H. Nhuyen and J. Fenton. Identification of roughness in open channels. *Advances in Hydro-science and engineering*, 3:111–119, 2004.
- [19] H. Oubanas, I. Gejadze, M. Pierre-Olivier, and M. Franck. River discharge estimation from synthetic SWOT-type observations using variational Data Assimilation and the full Saint-Venant hydraulic model. *Journal of Hydrology*, 559:638–647, 2018.
- [20] R. Ramesh, B. Datta, S. Bhallamudi, and A. Narayana. Optimal estimation of roughness in open-channel flows. *Journal of hydraulic engineering*, 126:3–13, 2000.
- [21] P. Roe. Approximate Riemann solvers, parameter vectors, and difference schemes. *Journal of Computational Physics*, 43:357–372, 1981.
- [22] H. Roux and D. Dartus. Sensitivity analysis and predictive uncertainty using inundation observations for parameter estimation in open-channel inverse problem. *J. Hydraul.Eng.*, 9:134–541, 2008.
- [23] M. Seller. Substrate design of reconstruction from free surface data for thin film flows. *Phys. Fluids*, 7:206–217, 2016.
- [24] J. Simon, J. Jeffrey, and K. Uhlmann. New extension of the Kalman Filter to nonlinear systems. In Ivan Kadar, editor, *Signal Processing, Sensor Fusion, and Target Recognition VI*, volume 3068, pages 182 – 193. International Society for Optics and Photonics, SPIE, 1997.
- [25] O. Soucek and Z. Martince. Iterative improvement of the shallow-ice approximation. *Journal of Glaciology*, 54:812–822, 2008.
- [26] Y. Spitz, J. Moisan, M. Abbott, and J. Richman. Data Assimilation and a pelagic ecosystem model: parameterization using time series observations. *Journal of Marine Systems*, 16(1):51–68, 1998.
- [27] J. Stoker. *Water waves*. Interscience Publishers, Inc, New York, 1986.
- [28] C. Vreugdenhil. *Numerical Method for Shallow Water Flow*. Kluwer Academic, Dordrecht, 1994.
- [29] R. Westaway, S. Lane, and D. Hicks. The development of an automated correction procedure for digital photogrammetry for the study of wide, shallow, gravel-bed rivers. *Earth surfaces processes and land forms*, 25:209–225, 2000.